ISSN 2176-5480

22nd International Congress of Mechanical Engineering (COBEM 2013)
November 3-7, 2013, Ribeirão Preto, SP, Brazil

DESIGN AND CALIBRATION OF A COMBUSTION CELL THOROUGHLY INSTRUMENTED FOR ANALYSIS OF SOLID WASTE CONVERSION AS ALTERNATIVE ENERGY SOURCE

Filipe Arthur Firmino Monhol[1]
Jaderson Nunes Pretti[2]
Universidade Federal do Espírito Santo - UFES, Av. Fernando Ferrari - 514, Goiabeiras, Vitória – ES, Brasil
filipe.monhol@gmail.com[1], jaderson13@hotmail.com[2]

Márcio Ferreira Martins[3]
Universidade Federal do Espírito Santo - UFES, Av. Fernando Ferrari - 514, Goiabeiras, Vitória – ES, Brasil
marciofm@ct.ufes.br[3]

Abstract. *With the constant rising demand for industrial energy and rising population it is necessary to study alternative energy sources as well as techniques to their conversion into useful work, at different consumption scales. The search for cleaner fuels, environmental preservation and the fact that humanity is producing increasingly solid waste, it requires recycling such waste energy, which can be performed satisfactorily through combustion. However, it is essential a detailed understanding of the combustion process, as well the operating variables. Therefore, this paper aims to design and to calibrate a versatile combustion cell, thoroughly instrumented, able to provide accurate data for studies "benchmark" the combustion process of different solid waste under different reactor configurations (co-current or counter-current). The cell consists of a stainless steel pipe with an insulating coating of ceramic material. A micro-sampling system to collect gas samples to determine the chemical structure of the front was designed. All measuring instruments are connected to a data acquisition system automated, allowing a continuous record of all experiments. It is possible to monitor the system through a graphical user interface generated by computational software.*

Keywords: *combustion, experimental device, waste, alternative energy, micro-sampling*

1. INTRODUCTION

The research development at the energy area shows that there are numerous possibilities for reuse of materials around us to produce alternative energy sources. Add the concept of recycling energy with decreasing waste, plus the desire to minimize harmful effects on man and nature and mainly to be economically feasible, are complex variables to linearize in order to obtain the best efficiency and utilization of those.

Humanity is increasingly producing solid waste, and in that there is a potential energy which cannot be neglected due to the large energy demand situation in which it is society. Among the residues are highlighted the plastic wastes and fecal human wastes, which are produced in high volume and present an energetic potential. The plastics are among the most discarded from the municipal solid waste, with a large percentage of the total mass collected and greatly impacting the environment. In the case of feces, existing technologies in the world for energy recovery of this waste is still very low, either by culture, lack of information or even by indifference. There is a culture that aversion to anything that refers to excrement, when in fact it is an energy source that can be reversed for the welfare of the man himself. Its availability is indisputable, and its energy potential, as shown in this work, is pretty high.

The alternative process design for the reuse of waste produced by various human beings is a challenge that has been researched hard by various institutions in various countries, with a desire to solve environmental problems and to achieve an efficient and highly profitable, which becomes a solution to the problem generated by the accelerated consumption of products for society.

The solid waste conversion as an alternative energy source has become possible through combustion. Combustion is one of the oldest technologies of the humanity and has been used for over a million years for different purposes. Despite the combustion be seen as a form of dirty energy production, it can be used consciously and clean without causing damage to nature. How is this possible? Just understand their characteristics and thermo-chemical processes, such that it can control it. The combustion will be only highly polluting if used without proper knowledge of their processes.

So, aiming to prevent this impending energy crisis due to growing global demand and the fossil fuels depletion, the performance of existing combustion systems need to improve further, and at the same time, reduce emission levels to meet international emissions standards. For this, a thorough and detailed study of the combustion is necessary.

1.1 Combustion front propagation

The combustion front propagation occurs in a variety of situations and for different purposes, such as waste incineration, gasification, in-situ combustion, sintering and other metallurgical processes burning solid fuels. The

ISSN 2176-5480

combustion front propagation description in a reactive porous medium remains a challenge for science in terms of physical chemistry and heat and mass transfer.

A pioneering work was done by Palmer (1957) who conducted a study about smoldering combustion in dust and fibrous materials. According Hobbs *et al.* (1993) the first major effort on the study of combustion front propagation dates from 1977 and 1979. Since then, environmental problems and the search for alternative energy sources has motivated further research on the subject. These efforts have focused on determining the parameters which influence the progress and the structure of a combustion front. To this end, some authors have developed numerical models and environmental devices (Ohlemiller, 1985).

The present work focuses on the study of the combustion front propagation in a porous medium by a reactive porous media device designed especially for this purpose. In this type of problem, the solid phase reacts with the gaseous phase resulting in various chemical reactions. Basically it is possible to distinguish three main areas of global reactions, each one characterized by an important step at the fuel conversion. *Drying zone*: As a result of heat transfer, the energy generated due to exothermic reactions from reactor parts, promotes the solid fuel drying. *Pyrolysis (Devolatilization) zone*: at temperatures above 250 °C it can occurs solid fuel pyrolysis, if there is a shortage in oxygen. Large molecules break down into molecules of medium size and fixed carbon. *Oxidation zone*: a burning (oxidation) zone is formed at the level where oxygen (air) is introduced. Reaction with oxygen is highly exothermic and results in a sharp increase at the temperature (1200 – 1500 °C).

This is a simplified approach, because in addition to oxidation, several other reactions (in order not always defined) occur in a combustion front, depending on the fuel and various other factors. It is therefore more appropriate to define a reaction zone rather than an oxidation zone. Figure 1 shows the regions possibly present in a fuel bed (with fixed carbon, volatile matter and some moisture) when propagating a combustion front. One can clearly observe the region where the reactions are more intense as well as the temperature variation and levels of O_2, CO_2 and carbon.

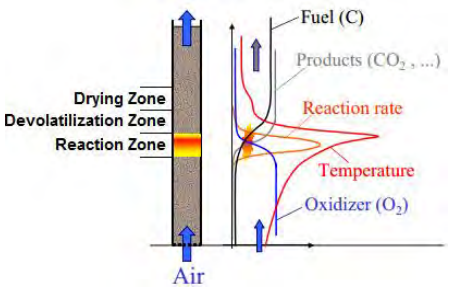

Figure 1. Zones possibly present in a fuel bed when propagating a combustion front (Debenest, 2003).

A front propagation can be by smoldering combustion or flaming combustion. The smoldering combustion is flameless combustion at low speeds and temperatures lower than flaming. The smoldering is sustained by the heat released in the surface oxidation of the fuel by oxygen. The propagation of a combustion front may also involve the phenomena related to the ignition of a homogeneous gas-phase reaction that is induced by a heterogeneous surface reaction (smoldering), which acts both in the production of gaseous fuel (pyrolyzed, CO, etc.) as the heat generation to start the reaction homogeneous, this situation is called flaming.

Thus, an important event can occurs and affect the combustion front shape, the passage from smoldering to flaming. The transition is most likely to occur when the heat released by the reactions (reactions in heterogeneous and homogeneous gas phase reaction) is greater than the heat loss to the surroundings (Bar-Ilan *et al.*, 2005). This author presents an experiment where the spread smoldering and transition to flaming are observed by the reduction of heat losses to the environment and the increase in oxygen concentration. Heat loss and oxygen availability are the most important parameters to be controlled in smoldering combustion trials.

There are two basic arrangements for the combustion front propagation: *counter-current combustion*, where the ignition advances in front of the fuel bed in opposition to the air supply. The provision of counter-current air is normally found in combustion processes in fixed bed. Application of counter-current combustion is incineration of solid waste (Ryu *et al*., 2006; Yang *et al*., 2005a; Yang *et al*., 2005b; Khor *et al*., 2007). In the second case, *co-current combustion*, the ignition advances in front of the fuel bed in the same direction as the air feed (Wang *et al.*, 2003; Thunman and Leckner, 2003; Bar-Ilan *et al*., 2004). The best example of co-current combustion can be found in-situ combustion for oil recovery (Castanier and Brigham, 2003; Akkutlu and Yortsos, 2003).

Few studies on co-current combustion were carried out so far. Wang *et al*. (2003) presented an experimental study of co-current smoldering combustion in horizontally forced forward condition. It was shown that the propagation of the front and its temperature increases with the rate of air flow.

Experiments in counter-current and co-current were studied by Thunman and Leckner (2003). The work focuses on the differences between these two arrangements. Thus, they investigated the effect of the ignition timing, the total time of conversion, the conversion zones position (pyrolysis, drying, firing) in time and along the length of the reactor.

ISSN 2176-5480

Pironi *et al*. (2009) performed co-current experiments smoldering combustion using a mixture of charcoal as a fuel in an inert medium, and obtained valuable information about the properties of the combustion front. Regarding the counter-current combustion process, several experimental devices have been developed for the combustion front propagation and structure investigation.

Vantelon *et al*. (2005) conducted an experimental study on co-current tires bed combustion and refractory briquettes. The authors found that the combustion process is influenced by the rate of air flow through the reactor. A combustion reaction with limited oxygen moves from a high residual oil production regime and low propagation speeds to a low regime oil production and conversion much faster.

Martins (2008) performed co-combustion in a stream bed of shale. Was developed a device similar to the one proposed in this work. Results regarding the geometry of the front, chemical structure, speed, among others was obtained.

Regarding the counter-current combustion process, several experimental devices have been developed for the combustion front propagation and structure investigation.

Gort *et al*. (1995) studied the air velocity and surface influence moisture content in three fuels: coke, wood and municipal waste shredded. The experiments were performed in a laboratory grate furnace.

Shin and Choi (2000) proposed a similar concept on the counter-current propagation of a combustion front using one-dimensional experiments. The air supply rate effects, the particles sizes and the fuel calorific value are discussed. Two fixed bed combustion modes can be distinguished based on the oxygen availability. *Oxygen-limited* combustion: At low air supply oxygen rates is completely consumed by carbon reaction and volatile material. In this case, the fuel reaction rate is determined by the oxygen supply rate. *Reaction-limited* combustion: If the air supply rate increases, combustion is increased, but due to the boundary existence of the combustion rate of the material within the bed, there is an increase of oxygen concentration in the output. In this case, the reaction rate cannot increase due to further reaction rate limit and, therefore, may be noted the bed cooling by air convection.

Liang *et al*. (2008) reported another important aspect concerning the solid particles composition heterogeneity. For the sample extracted in different parts of corn straw, the concentration of CO and NO are clearly different. According to the author, the corn straw combustion occurred in two stages: the propagation of the front ignition and oxidation Char. Both stages were identified by Thunman and Leckner (2005), Zhou *et al*. (2005) and Ryu *et al*. (2006).

2. WORK OBJECTIVES

The main work objective is to design a combustion cell for different solid fuels types, which will allow the realization of a geometric description of the different zones that make up a combustion front. It may obtain the temperature levels reached in the bed, reducing pressure in the bed, the composition of the gases generated by front, the profile of the combustion front propagating within the bed, temperature losses to the environment as well as several other factors.

With the device proposed in this work it can be performed both types mentioned combustion, thus allowing a thorough combustion study processes available in both co-current and in counter-current. These results, along with a physical chemistry and thermal characterization of the products and ashes will be a comprehensive reference, allowing the modeling process in future work.

To operate the combustion in the porous medium in this cell and in a controlled manner, the experimental device was calibrated using various solid fuels. Since there are few studies in co-current combustion, priority will be given to this in the present work to obtain scientific data relevant to the demand.

3. EXPERIMENTAL DEVICE

All works cited above utilize a vertical cylinder with an inside diameter between 15 cm and 24.4 cm and a chamber height between 30 cm and 150 cm, and all are wrapped with insulating material layer. The temperature measurements are made using thermocouples placed on the shaft at different times. The mass put inside the bed is sometimes measured by using a weighing scale. The flue gases are usually analyzed in the cell output.

The French Standards Association (AFNOR) published the standard NF M03-049, which deals with solid fuels characterization in a fixed bed in counter-current flow. The norm is based on measuring the combustion front speed, the combustion rate, pressure drop and temperature. According to the standard, the reactor should preferably have a cylindrical shape with a diameter of not less than 25 cm, in order to prevent excessive influence on the results wall.

The experimental device, developed in the present work, is similar to that developed by Martins (2008) and was developed for conducting experiments 1-D co-current or counter-current. The Fig. 2, Fig. 3 and Fig. 4 show a mounting arrangement for a co-current experiment.

The cell bed consisting of a stainless steel vertical cylinder, inner diameter of about 73 mm and height 450 mm. The diameter is designed large enough to limit the heat loss through the walls, while narrow enough to prevent the preparation of large experimental samples. The cylinder is surrounded by two types of thermal insulation materials: 3 mm thermal blanket (blanket Superwool 607, Thermal Ceramics, thermal conductivity of 0.28 $Wm^{-1}K^{-1}$ at 982 °C) and

ISSN 2176-5480

46 mm thick refractory fibers (Kaowool 45 HS Board, Thermal Ceramics, thermal conductivity of 0.21 $Wm^{-1}K^{-1}$ at 1000 °C). The grid is located at the chamber bottom and consists of a stainless steel mesh. It is supported by an inner ring, which in turn is supported by reactor cone bottom. At the cell bottom is placed a flexible silicone tube attached to bubblers to collect the condensate, and gas exits through the exhaust system. The air intake is designed to provide uninterrupted air flow in a symmetrical manner.

The reactor is thoroughly instrumented. A group of eight in-line thermocouples 1.5 mm in diameter and 122 mm length (T1, T2, T3, T4, T11, T12, T13, T14) are located at Z = 0, 45, 90, 135 and 225 , 270, 315, 360 mm (measured from top to bottom of the reactor), allowing to measure temperature along the axis of the cell at different heights. A crown of six thermocouples same as described above, but 95 mm in length (T5, T6, T7, T8, T9, T10) allows measuring the temperature along a horizontal plane (at middle height, Z = 180 mm) 6.5 mm away from the wall. This arrangement will reveal whether the combustion front progresses or not a horizontal surface. The gas analyzer with real-time acquisition can be connected to two different points, one lying on the bottom of the reactor and the other is at the same height of the thermocouples crown. The pressure at the top of the reactor and the temperature along the bed is continuously recorded and monitored via computational software.

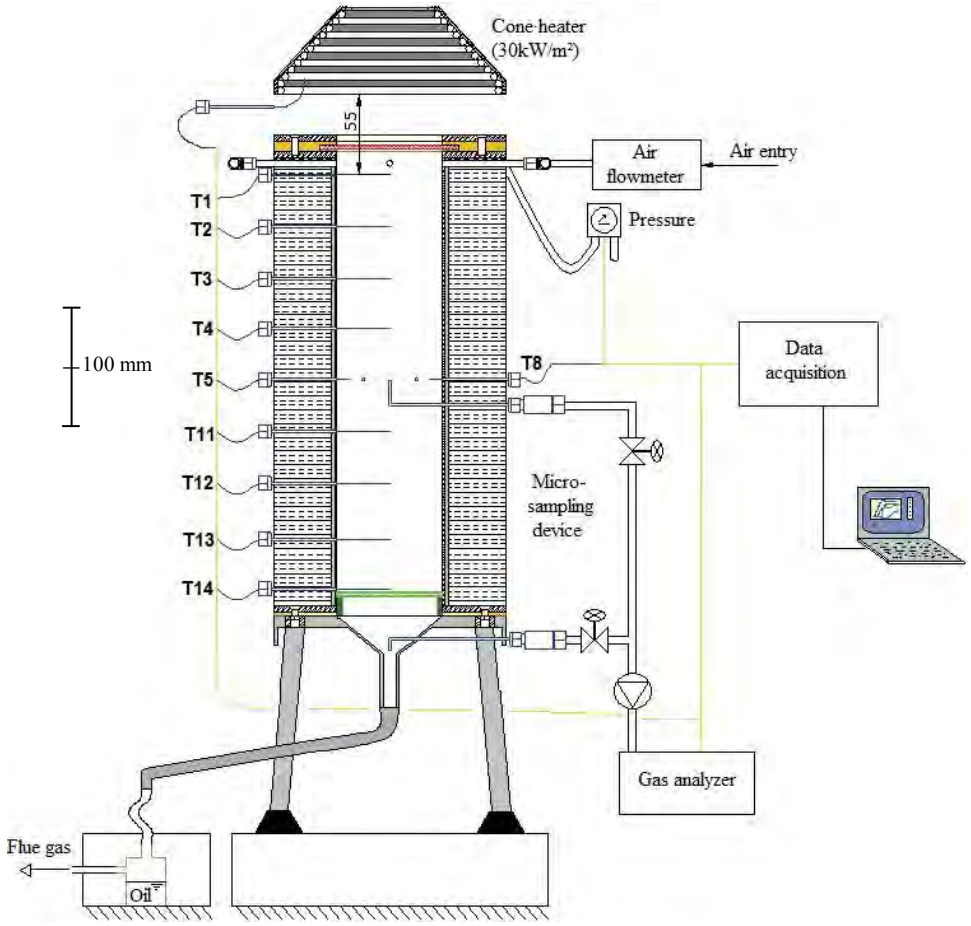

Figure 2. Combustion cell developed with micro-sampling system and data acquisition.

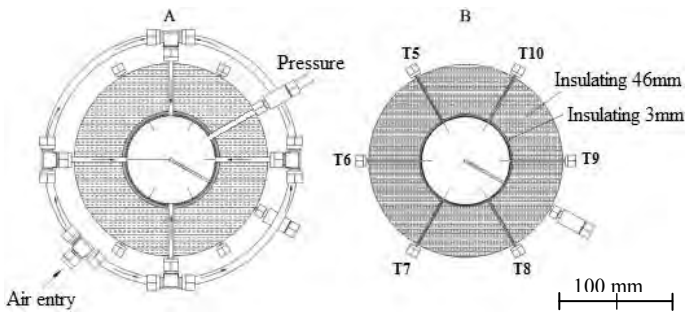

Figure 3. Cross section at the reactor top (A) and at the crown of thermocouples (B).

ISSN 2176-5480

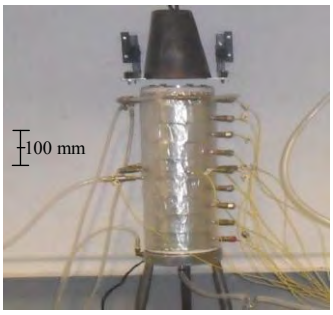

Figure 4. Cell photo.

3.1 Ignition of the combustion

To start a uniform front across the whole surface of the bed, a sophisticated ignition device called Cone Calorimeter was developed. A radiative flux is generated by a metal surface called a cone heater. On the ignition time, the radiant cone heater temperature is adjusted to 570 °C to impose a heat flux of 25 to 30 kW m−2 over the top surface of the solid fuel. The radiative flux crosses a quartz porthole that ensures the sealing of the closure. The solid fuel inside the cell is located 50 mm from the cone. The cone had been previously calibrated by measuring the temperature in a plane 50 mm below the cone, to obtain the temperature distribution which would be acting on the fuel top surface at the time of ignition. The temperature at about 50 mm from the cone (on the fuel top surface) is given by the interpolated surface in computational software via the temperature data collected; see Fig. 5. The heating time of the cone is about 15 minutes.

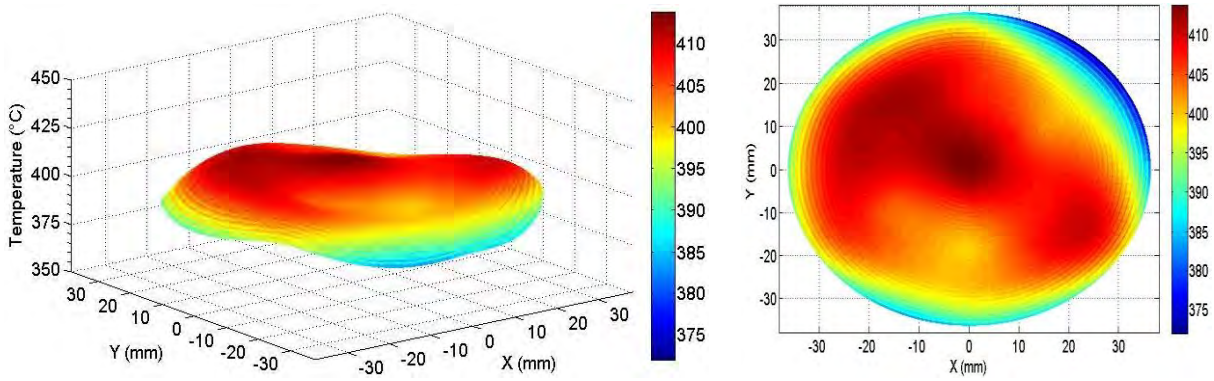

Figure 5. Temperature Surface generated by the cone at 50 mm of distance.

3.2 Micro-sampling system and gas analyzer

An innovative system is designed and configured to improve the physical and chemical structure front. The micro-sampling system is shown in Fig. 1 and in Fig. 2. This system has the capability of micro-gas sampled at two points inside the cell, at the mid- height and output cell.

Sampling may be performed before, during and after the passage of the combustion front. At the mid- height, the sample is collected through a tube of internal diameter 1.6mm. The sampled flow rate should be set so that it is isokinetic the air flow within the bed so as to minimize front disruption. At the output cell, the sample is collected through a face down pipe (diameter of 3 mm) in order to prevent the condensed entry. The gas of sample points is conducted to the gas analyzer that measures the volumetric percentage of the gaseous products of combustion O_2, CO, NO, NO_2, CxHy, NOx and H_2 with the aid of electrochemical cells, and the volumetric percentage of CO_2, with the aid an infrared cell.

4. COMBUSTION CELL CALIBRATION USING DIFFERENT SOLID WASTE MATERIALS

Five different experiments were performed to calibrate the cell combustion thoroughly instrumented developed for this work. Due to the great importance of fecal and plastics waste, as previously mentioned, in addition to Charcoal, the Polyethylene and Human feces waste were used as fuel for calibration. All combustible materials were ground, sieved and dried. Table 1 shows each experiment features. Before each experiment, a tightness test was performed pressurizing the equipment above the operating pressure. Thus can be ensured that the air flow measured by the flow meter not miss it for possible leak points.

ISSN 2176-5480

Table 1. Parameters of the experiments.

Experiment	Feedstock	Total mass (kg)	Mass ratio	Air flow (kg/h)	Granulometry (mm)
1	Charcoal/Polyethylene	0.6146	10:2	0.676	2 (both)
2	Charcoal	0.6527	1	0.676	2
3	Charcoal	0.6522	1	0.151	2
4	Human feces	0.8652	1	0.676	5
5	Charcoal/Sand	1.9410	3:20	0.676	2 (both)

The air flow rate of the experiments 1, 2, 4 and 5 corresponds to a Darcy velocity of 0.024 m s^{-1} at 20.0 °C, or 0.173 m s^{-1} at 1000 °C. The experiment 3 was run with an air flow rate that corresponds to a Darcy velocity of 0.0075 m s^{-1} at 20.0 °C, or 0.054 m s^{-1} at 1000 °C.
Table 2 shows the average temperature in the bed and the duration of each experiment.

Table 2. Average temperature and the duration of each experiment.

Experiment	Time (min)	Temperature (°C)
1	294	925
2	266	1119
3	2175	906
4	195	885
5	169	1188

In the case of charcoal (experiments 2, 3 and 5) the temperature in the experiment with sand is greater, this may be explained by the fact that the sand has a greater ability to retain heat, causing heating of the air before reaching the combustion front. In experiments 2 and 3 the air reaches the combustion front at a low temperature resulting in a lower flame temperature, considering that the bed has been extinct in the region where the combustion front has passed. Furthermore, it is observed that for a very low flow the time is greater and the temperature still remains close to 1000 °C, which indicates that it can generate power for a longer time using lower flows.

5. TEMPERATURE RESULTS

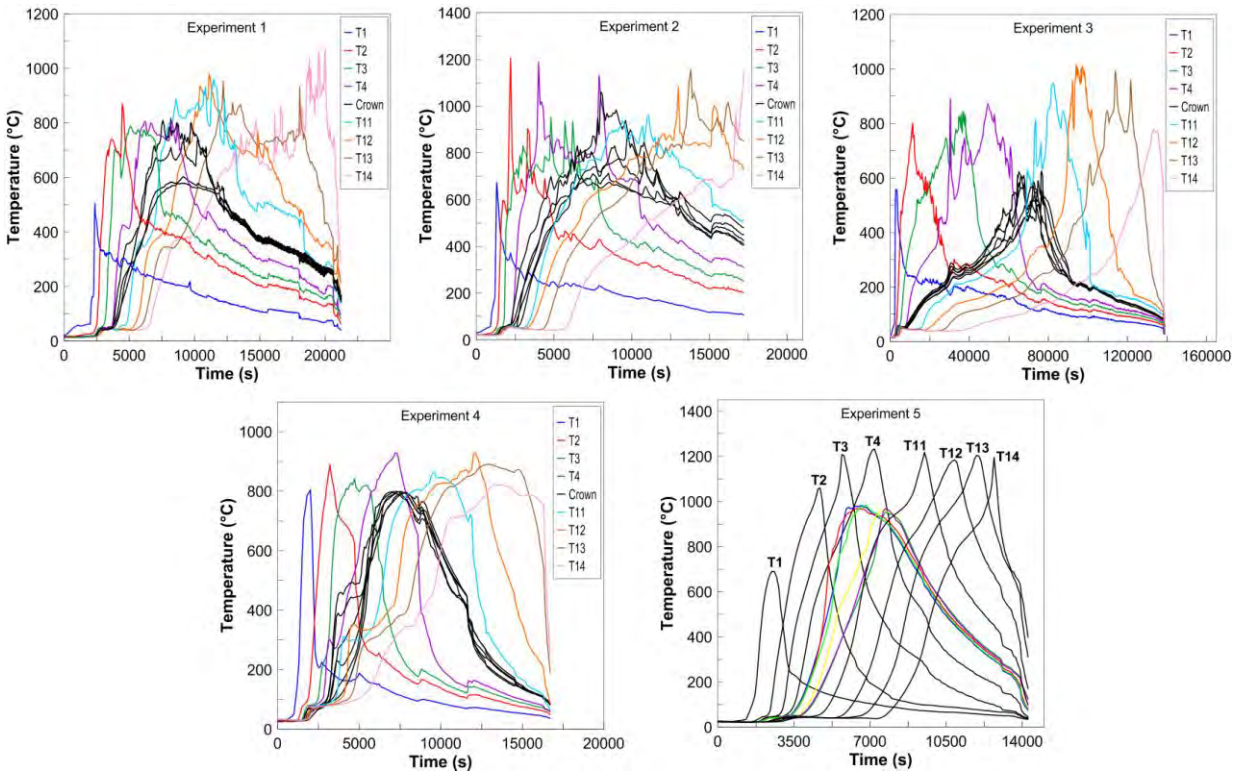

Figure 6. Temperature evolution of the thermocouples placed along the axis and placed at horizontal cross section (the profiles of axial termocouples are clearly distinguishable in the Experiment 5, so were not distinguished by color).

ISSN 2176-5480

The temperature values obtained at different locations within the bed for each experiment are illustrated in Fig. 6. It can be observed that the experiments using charcoal with a high mass fraction (Experiments 1, 2 and 3) are highly collapsing since the bed is consumed and collapses after oxidation of charcoal. Thus, these experiments show a instability in temperature profiles far superior to less collapsing experiments (Experiments 4 and 5), requiring special techniques such as curve fitting and determining the weighted average of the peak region for the location of peak temperature for each thermocouple and calculating the velocity of the combustion front.

On the horizontal cross section at mid-point of the height of the bed (Crown - T5 to T10) in all experiments can be seen that the peak temperatures were significantly lower peaks along the axis of the cell. This shows that the assumption of a purely 1D not been achieved, which can be attributed to significant heat loss through the walls of the cell. This observation indicates that in the literature experiments where the combustion front is observed in reactors without isolation of smallest diameter, the heat losses were probably much higher and significantly affect the structure of the combustion front. The reader can find detailed experimental and theoretical work about the effect of heat losses on opposed smoldering, and on critical conditions to achieve a self sustaining combustion front, both in microgravity and in ordinary gravity (Bar-Ilan *et al*., 2004).

Figure 7 shows axial temperature profiles along the reactor axis at different times for the Experiment 5. These profiles were obtained by plotting – at the peak time for each thermocouple – the temperature values for all thermocouples. The front velocity was used to calculate the position *Z* of the thermocouple relative to the Temperature Peak Point (TPP) at each time. The temperature decrease downstream of the TPP (right hand side of TPP) keeps quite a constant shape at different times, while the hot zone upstream of the front becomes larger as the front progresses.

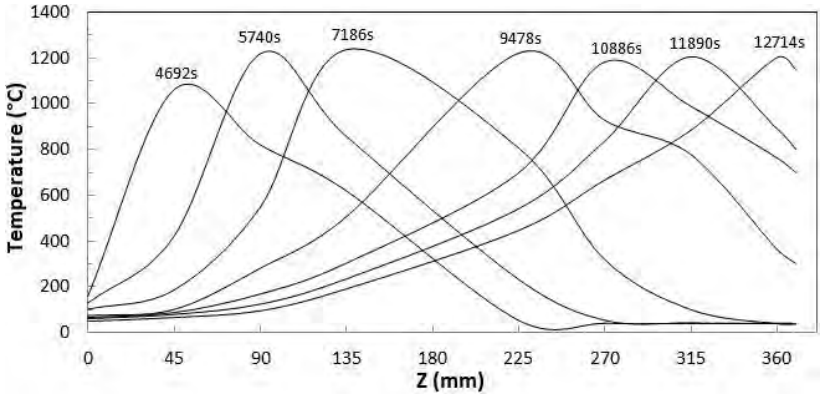

Figure 7. Axial temperature profiles along the axis of the cell at different times.

6. COMBUSTION FRONT

6.1 Front velocity

The combustion front velocity is determined from the data generated by the passage of the front at each thermocouple in the cell axle. A quadratic polynomial function giving the position of the combustion front versus time was fitted to the experimental points, see Fig. 8-a. The r^2 ranged from a minimum of 0.991033 (for the fourth experiment) to a maximum of 0.998171 (for the fifth experiment), indicating that the curves were almost perfectly adjusted. The time derivative of this function is the velocity of the combustion front, as shown in Fig. 8-b. It can be observed that, in general, for the experiments that were not very instabilities due to the constant falls from the bed, the velocity is an increasing function (experiments 4 and 5). Al-Saffara *et al*. (2000), Torero and Fernandez-Pello (1996) and Martins (2008) found a similar trend.

A probable explanation for the velocity evolution is a progressive change in the molar CO/CO_2 ratio produced by fixed carbon oxidation, which means a decrease in CO_2 production in favor of CO production. This enables the oxidation of a greater number of carbons with a given amount of O_2 (Martins, 2008).

However, in unstable experiments, that is where the falling bed was constant due to the front passage (experiments 1,2 and 3), the instabilities cause changes in the velocity profiles in order to slow down the combustion front. This can be clearly observed in experiments 1 and 2. In experiment 1, the region with higher instability due to falls from bed, is the final region and in experiment 2 the region with the highest instability is the initial region. In these most unstable regions there is a slowdown in speed. This deceleration can be identified by concave down - if fit a local curve - of the points (position versus time) in these regions.

In experiment 3, there is a characteristic drop in the bed - lowering the temperature T3 and increasing the temperature T4, see Fig. 6 at the time around 30000 s. It can be noted that in this region there is a slowdown in the front velocity by observing the points (position versus time) of the experiment, see Fig. 8-a. Thus, in experiments where there was excessive falls the bed velocity follows a decreasing profile, see Fig. 8-b.

ISSN 2176-5480

The velocity in experiment 3 behaved almost constant, although it behaved decreasing, this is due to the very low air flow and the inevitable, but smaller compared to experiments 1 and 2, falls on the bed. However there is equilibrium between the velocity deceleration due falls from the bed and its normal tendency to accelerate, as shown in more stable bed (experiments 4 and 5). This indicates that as the falls from bed slow down the front velocity and CO/CO_2 ratio tends to accelerate it, the flow rate of 0,151 kg h^{-1} is close to the balance between these two factors, i.e., this flow rate is necessary to cancel the factors that accelerate and decelerate the combustion front and keep it at a constant velocity.

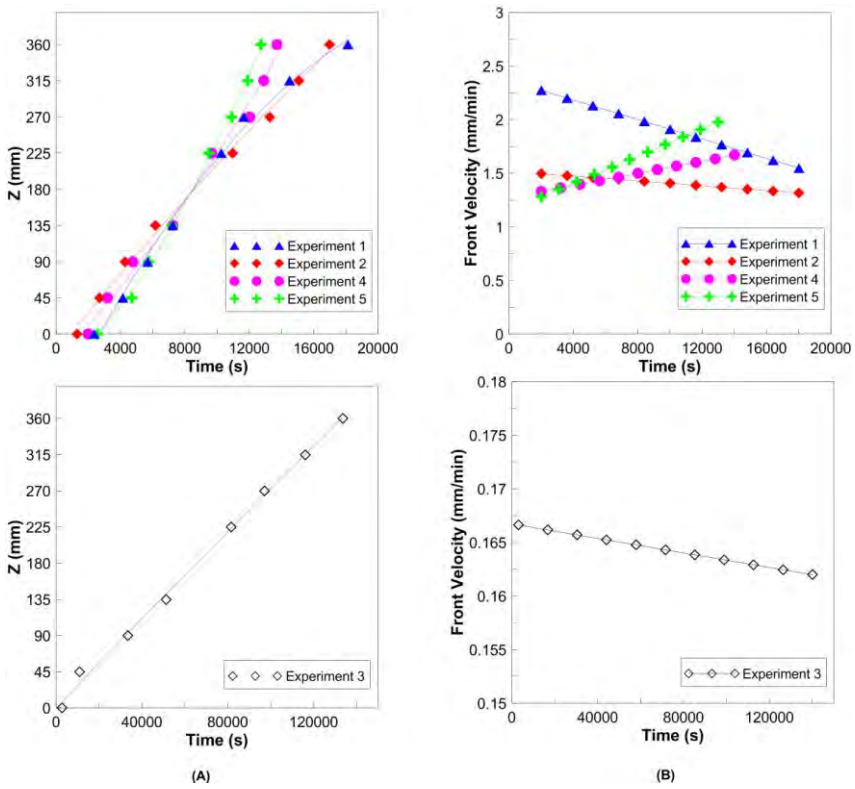

Figure 8. (a) Curve fitting to the experimental points (Z x time). (b) Combustion front velocity.

6.2 Thermal structure of the combustion front

From the temperature profile at a given time, a first geometrical description of the front structure can be established. For example, for the fifth experiment, Fig. 9 shows the axial temperature profile along the reactor to peak time of the thermocouple 5 (7186 s), where Z was fixed to 0 at the TPP (Temperature Peak Point).

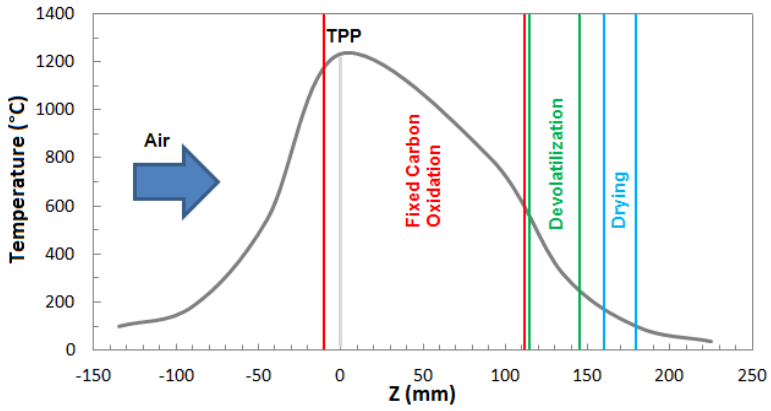

Figure 9. Front structure evaluated from temperature profile.

Figure 9 shows the geometric description of the front structure:

- If one assumes that drying becomes very fast and is completed rapidly when the temperature reaches 150 °C, the drying zone can be localized downstream of the TPP, starting 180 mm from the TPP as illustrated in

ISSN 2176-5480

Fig. 9. Can affirm the existence of this zone due to moisture present in the charcoal used, which was confirmed by weighing the water in bubblers at the end of the experiment (about 5% moisture). The length of the drying zone was about 20 mm. This zone increases as the water is accumulated in the lower parts of the cell.

- Devolatilization can be assumed to progress significantly as the temperature reaches 250 °C, and to be very fast at 550 °C. Consequently, the devolatilization zone can be localized between 115 mm and 145 mm downstream the TPP; its thickness is about 30 mm. According to the gas analysis, charcoal in question was not just made up of fixed carbon, but also possessed a considerable percentage of volatile material in its composition (well above 5%, which was the limit of measurement of the CxHy electrochemical cell), which explains the existence of this zone.
- For fixed carbon oxidation to occur, the temperature must be higher than 550 °C, and oxygen must be present. Air is fed from upstream of the combustion front, and a relevant percentage of O_2 are still present at the exit of the cell. The zone where the two criteria are satisfied ranges from negative values of Z to Z = 115 mm. Nevertheless, at negative values of Z, there is probably no more fixed carbon present. It is not possible at this stage to localize where the oxidation has the highest rate, although this is probably around the TPP. The great extent of this zone is consistent with the expected due to the fact that charcoal is primarily composed of fixed carbon.

6.3 Shape of the front

The Fig. 10 illustrates the combustion front surface generated for the experiment 5 with the aid of computational software the instant at which the combustion front is located approximately at the same height in the thermocouples crown. This surface was obtained through the peak times of each thermocouple crown and using the front velocity to find the position of each point at the average time of the front passage through the crown thermocouples.

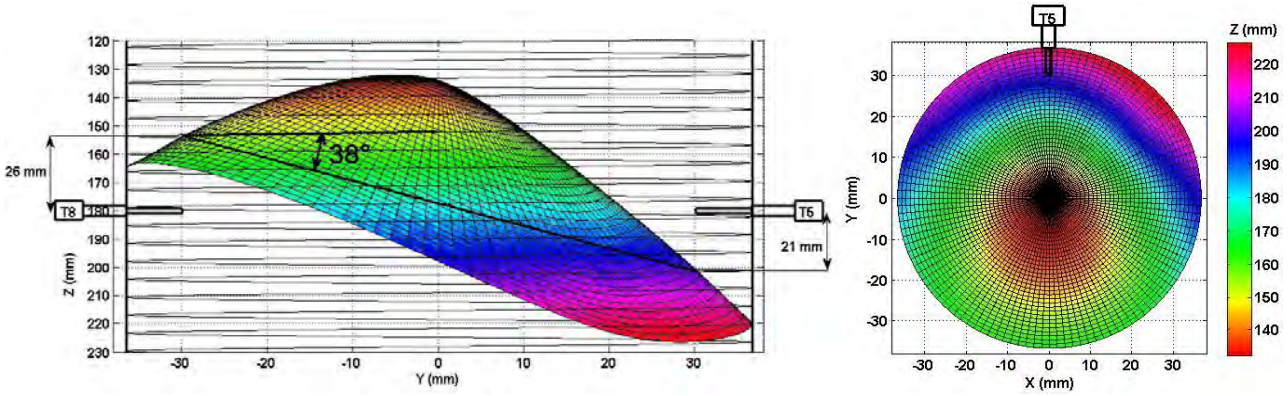

Figure 10. Shape o f the front.

Noting this surface can be noted that front propagation in the experiment is not horizontal but inclined (38°), and propagates more rapidly in the periphery of the bed. Furthermore, looking at the Fig. 6 results (for the Experiment 5), it is clear that the front reached the first crown thermocouple before than the cell axis in the same height Z of the bed. This result confirms that the front is not a flat surface but a curved surface with the top on bed symmetry axis.

The fact that the front does not propagate uniformly can be a result of non-uniform radiative flux heat during ignition. Instabilities due to the ignition process or heat loss through the walls may also contribute to the inclination of the front and non-uniformity of the shape. Another possible explanation for the faster progress of the front in the cell walls can be the O_2 supply as demonstrated by Martins (2008). The mass flow of O_2 near the cold wall is possibly higher than in the axis, because: (1) The O_2 density is higher on the walls, due to the lower temperature; (2) The viscosity is smaller, also because the lower temperature; (3) The particles arrangement in contact with the walls is not as dense as the cell rest.

7. GAS ANALISYS

The *chemical thickness* of the front can be also investigated using the micro-sampling system. The gas composition at different locations of the combustion front can be found. This enables a considerable understanding of the reactions present in front. These studies can be performed with the system designed in this work.

Gas analysis was performed for the experiments 2, 3, and 4. The results are preliminary. Some components, such as CxHy, NOx, NO and NO_2 could not be measured successfully. Therefore the system can be optimized later.

ISSN 2176-5480

At the cell exit, curves obtained are shown in Fig. 11. It is observed that there are two combustion systems present in the cell. At the experiment beginning there is a tendency for *oxygen-limited* combustion, since the amount of oxygen in the outlet is zero or close to zero, indicating that the oxygen is completely consumed. Thus, the fuel reaction rate is determined by supply of oxygen. At the experiment end there is a *reaction-limited* combustion, since oxygen is present in considerable amounts in the cell output. This is due to the existence of the combustion rate limit of materials within the bed, resulting in increased oxygen concentration in the output. In Experiment 4 was possible to perform a more complete analysis of the gas constituents in the cell output, worth remembering that considerable amounts of CxHy (well more than 5%) were also present. However, it was not possible to measure them due to the limit of the CxHy electrochemical cell have been exceeded. Thus, the electrochemical cell must be replaced by a larger measurement range, if it is desired to measure the amount of this component during cell operation. Note also that there is a high concentration of CO, which may be due to devolatilization reactions. However, these reactions do not produce as much CO, it can be assumed that also occurred gasification reactions in the bed. The presence of hydrogen in considerable quantities reinforces this hypothesis. The presence of hydrogen can also be due to moisture in the fuel and air supply.

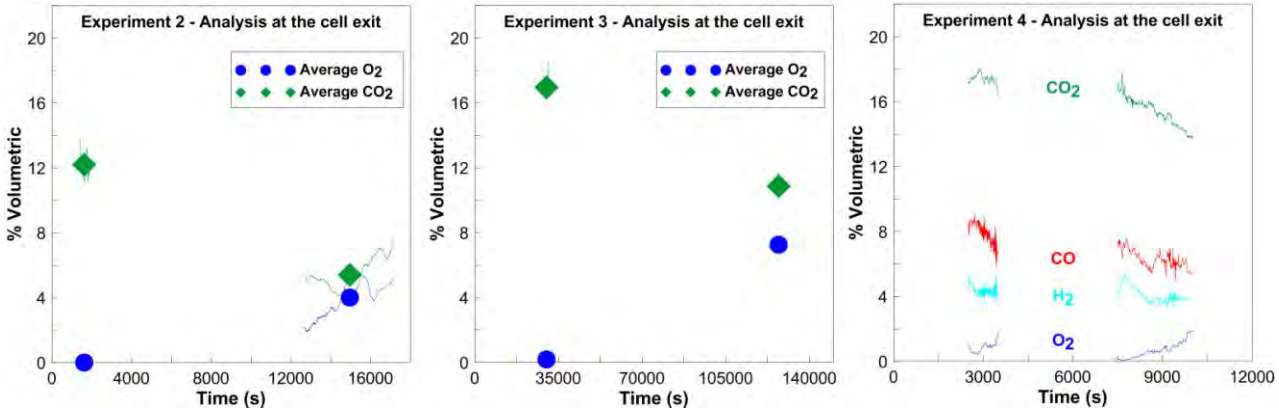

Figure 11. Results of gas analysis at the cell exit.

At the crown were found curves shown in Fig. 12 to the experiment 2 and 3.

In Experiment 2 there was a large variation in the oxygen and carbon dioxide amounts, which may be due to the bed portion collapsing upon Micro-sampling System, since the peaks of CO_2 formed at the same time that occurred temperature peak in the thermocouple near Micro-sampling system. It was observed that at the intervals of CO_2 peaks and O_2 valleys, or at times that the combustion reactions are occurring at the micro-sampling system entrance, there was a *reaction-limited* combustion, which can be confirmed by oxygen present in substantial amounts (about 5%).

In experiment 3 the sampling was done long before the front to reach the crown, so the results are quite stable. The total oxygen consumption by the front, which is just above the gas sampling, indicates that at the experiment beginning there truly is an *oxygen-limited* combustion, as previously stated.

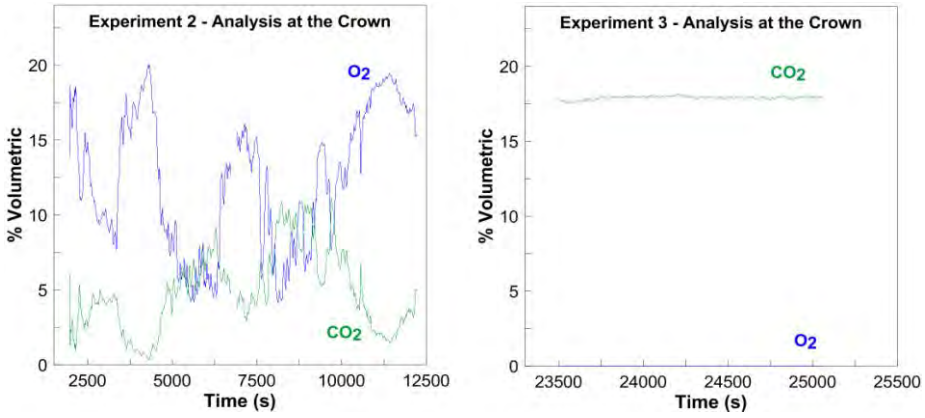

Figure 12. Results of gas analysis at the cell middle.

8. PRESSURE AT THE COMBUSTION CELL TOP

As shown in Fig. 13, for most experiments, first the pressure at the bed top gradually increases to a certain value. After this, it can be observed a decrease in pressure as the temperature increases in below thermocouples. The

ISSN 2176-5480

progressive increase might be explained by two phenomena: (i) The temperature increase of the medium; (ii) the progressive formation of a condensed bank at downstream of the combustion front, or the clogging of the medium by condensed deposits and porosity decrease. The sudden decrease can also be explained. It is clearly observed that the pressure drop occurs shortly after the temperature increase at the cell bottom, which is just when the condensed volatile reach this region and are evacuated. Thus, the pressure in the bed is relieved. It is also observed that this phenomenon occurs in more than one step for experiments 1 (charcoal and pet) and 4 (feces). This is due to the fact that there are for these two experiments a wider variety of substances, with different reactions in the bed. The first increase and subsequent drop in pressure is due to the lighter volatiles were carried by the bed and then evacuated at the outlet, and the second is due to the same process for heavier volatiles.

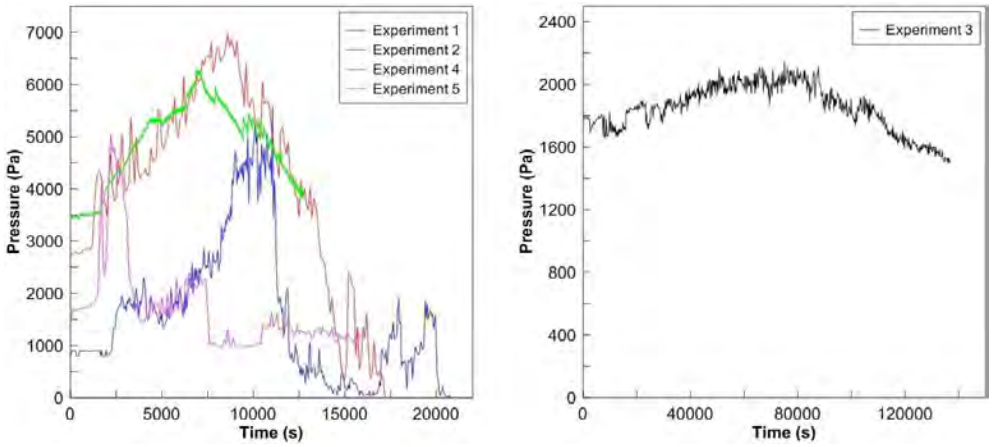

Figure 13. Pressure evolution in the bed.

The experiment 4 showed a peak and drop of pressure in the lowest temperature at the cell bottom, it indicates that the feces have a high content of volatile lighter. The pressure instability in the experiments is due to momentary blockage of the cell exit and of the medium by a condensate bank that is being adduced at downstream. The peaks at the end of the experiments 1 and 2 are due to other factors, such as, for example, falls from the bed that was left behind without being totally consumed, which restarts the condensate production process and cell outlet obstruction. It may also be due to the fact that in these two experiments the duct, present in the cell exit, failed due to the increase in temperature. The pressure in Experiment 3 remained at lower values due to the fact that the air flow and the reactions velocity are much smaller.

9. CONCLUSION

The experiments gave significant results. By using inert medium (sand) the temperatures reached are higher due to preheat the air by inert medium that has greater capacity to retain heat. By using lower flow rates can get higher amount of energy available in the external walls of the reactor. The advance of the front is dependent on the supply of air. Their geometry tends to be non-uniform with slight inclinations and propagates faster in the periphery of the bed due to factors such as the ignition process instability or loss of heat through the walls, resulting in increased O_2 supply near the walls.

Despite the relatively large diameter of the cell and a good thermal insulation, heat losses are significant in relation to the heat generated by combustion.

The micro-sampling system identifies the gases inside the front and allows characterize it geometrically and chemically. There was a tendency to the emergence of two combustion systems in the cell. At the beginning there is *oxygen-limited* combustion and at the end *reaction-limited* combustion.

The front velocity is an increasing function. However, in beds where constant collapses occur, due to their passage, it becomes decreasing. Falls in the bed, due to the formation of ashes, slow the front considerably.

From the set temperature profiles, can be made the geometry of the drying, devolatilization and oxidation zone, if they exist, as well as others which happen to exist depending on the fuel used.

The pressure within the bed tends to increase due to the accumulation of condensate. When the condensates reach the end of the cell and are evacuated causes the pressure decreases.

Thus, by means of this new experimental device one-dimensional study of combustion front propagating to different waste fuels with air supply co-current and counter-current can be studied in a complete manner. Although focus is given to the co-current arrangement, for which the results were obtained in a satisfactory manner, the cell also enable future studies in counter-current arrangement, considering that was also designed for this type of propagation.

ISSN 2176-5480

10. ACKNOWLEDGEMENTS

This work was partly supported by the PRH-29 program through the research project developed by the Laboratório de Combustão e Combustíveis - UFES - Brazil. The authors wish to thank them here.

11. REFERENCES

Akkutlu IY, Yortsos YC., 2003. "The dynamics of in-situ combustion fronts in porous media". *Combustion and Flame* 134 (3): 229–47.

Al-Saffara H, Priceb D, Soufia A, Hughesa R., 2000. "Distinguishing between overlapping low temperature and high temperature oxidation data obtained from a pressurised flow reactor system using consolidated core material". *Fuel* 79 (7): 723–32.

Bar-Ilan, A., O.M. Putzeys, G. Rein, A.C. Fernandez-Pello, and Urban D.L., 2005. "Transition from forward smoldering to flaming in small polyurethane foam samples." *Proceedings of the Combustion Institute* 30 (2): 2295-2302.

Bar-Ilan A, Rein G, Fernandez-Pello AC, Torero JL, Urban DL., 2004. "Forced forward smoldering experiments in microgravity". *Experimental Thermal and Fluid Science* 28 (7) : 743–51.

Castanier LM, Brigham WE., 2003. "Upgrading of crude oil via in situ combustion". *Journal of Petroleum Science and Engineering* 39 (1–2): 125–36.

Debenest G., 2003. *3D microscale numerical simulation of oil shale combustion in fixed bed*. Ph.D. thesis, University of Poitiers, Poitiers.

Gort R, Valk M, Brem G., 1995. "Solid fuel combustion in a laboratory grate furnace". In: *Proceedings of third AsianPacific symposium on combustion and energy utilization*. Hongkong;.

Hobbs ML, Radulovic PT, Smoot LD., 1993. "Combustion and gasification of coals in fixed-beds". *Progress in Energy and Combustion Science* 19 (6): 505–86.

Khor A, Ryu C, Yang YB, Sharifi VN, Swithenbank J., 2007. Straw combustion in a fixed bed combustor. *Fuel* 86 (1-2): 152–60.

Liang L, Sun R, Fei J, Wu S, Liu X, Dai K., 2008. "Experimental study on effects of moisture content on combustion characteristics of simulated municipal solid wastes in a fixed bed". *Bioresource Technology* 99 (15): 7238–46

Martins M. F., 2008. *The structure of a combustion front propagating in a fixed bed of crushed oil shale: co-current configuration*. Ph.D. thesis, University of Toulouse, Toulouse.

Ohlemiller TJ., 1985. "Modeling of smoldering combustion propagation". *Progress in Energy and Combustion Science* 11 (4) : 277–310.

Palmer KN., 1957. "Smouldering combustion in dusts and fibrous materials". *Combustion and Flame* 1 (2): 129–54.

Pironi P, Switzer C, Rein G, Gerhard JI, Torero JL, Fuentes A., 2009. „Small-scale forward smouldering experiments for remediation of coal tar in inert media". *Proceedings of the Combustion Institute* 32 (2): 1957-1964.

Ryu C, Yang YB, Khor A, Yates NE, Sharifi VN, Swithenbank J., 2006. "Effect of fuel properties on biomass combustion: part I. Experiments – fuel type, equivalence ratio and particle size". *Fuel* 85 (7–8): 1039–46.

Shin D, Choi S., 2000. "The combustion of simulated waste particles in a fixed bed". *Combustion and Flame* 121 (1–2): 167–80.

Thunman H, Leckner Bo., 2003. "Co-current and counter-current fixed bed combustion of biofuel – a comparison". *Fuel* 82 (3): 275–83.

Thunman H, Leckner B., 2005. "Influence of size and density of fuel on combustion in a packed bed". *Proceedings of the Combustion Institute* 30 (2): 2939–46.

Torero JL, Fernandez-Pello AC., 1996. "Forward smolder of polyurethane foam in a forced air flow". *Combustion and Flame* 106 (1–2): 89–109.

Vantelon J-P, Lodeho B, Pignoux S, Ellzey JL, Torero JL., 2005. "Experimental observations on the thermal degradation of a porous bed of tires". *Proceedings of the Combustion Institute* 30 (2): 2239–46.

Wang JH, Chao CYH, Kong W., 2003. "Experimental study and asymptotic analysis of horizontally forced forward smoldering combustion". *Combustion and Flame* 135 (4): 405–19.

Yang YB, Ryu C, Khor A, Yates NE, Sharifi VN, Swithenbank J., 2005a. "Effect of fuel properties on biomass combustion. Part II. Modelling approach – identification of the controlling factors". *Fuel* 84 (16): 2116–30.

Yang YB, Ryu C, Khor A, Sharifi VN, Swithenbank J., 2005b. "Fuel size effect on pinewood combustion in a packed bed". *Fuel* 84 (16): 2026–38.

Zhou H, Jensen AD, Glarborg P, Jensen PA, Kavaliauskas A., 2005. "Numerical modeling of straw combustion in a fixed bed". *Fuel* 84 (4): 389–403.

12. RESPONSIBILITY NOTICE

The authors are the only responsible for the printed material included in this paper.